FIRST RESULTS FROM THE NOMAD EXPERIMENT AT CERN (SEARCH FOR $\nu_\mu \rightarrow \nu_\tau$ OSCILLATIONS)

THE NOMAD COLLABORATION

presented by

Boris A. Popov

LPNHE, Universités Paris VI et Paris VII,
4, place Jussieu, Tour 33 Rez de Chaussée,
75252 Paris Cedex 05, France

Permanent address:
Laboratory of Nuclear Problems,
Joint Institute for Nuclear Research,
141980, Dubna, USSR

NOMAD is a neutrino oscillation experiment designed to search for ν_τ appearance in the CERN-SPS wide band predominantly ν_μ beam. Signal detection is based on the identification of ν_τ charged current interactions with the help of kinematic criteria. After the completion of the detector in August, 1995 the experiment has been successfully taking data till the end of 1996. The detector performances are in good agreement with our expectations. Preliminary analysis based on the 1995 data sample allows NOMAD to achieve the limit of 4×10^{-3} on $\sin^2 2\theta_{\mu\tau}$ for large Δm^2. NOMAD will continue to run during 1997. If no evidence for oscillations is found in all the NOMAD data the sensitivity to the oscillation parameters is expected to be improved by an order of magnitude with respect to the current limit.

1 Introduction

The Neutrino Oscillation MAgnetic Detector (NOMAD, WA-96) experiment [1] was designed to search for ν_τ appearance from $\nu_\mu \rightarrow \nu_\tau$ oscillations in the CERN-SPS wide band neutrino beam.

In the absence of oscillations the relative beam composition in $\nu_\mu : \bar{\nu}_\mu : \nu_e : \bar{\nu}_e$ is 1 : 0.07 : 0.01 : 0.003 with average energies of 23.6, 22.7, 37.1 and 33.2 GeV respectively (Fig. 1). Prompt ν_τ's come from the reaction $p\mathcal{N} \rightarrow D_s X$ with subsequent decays of $D_s \rightarrow \tau\ \nu_\tau$ and $\tau \rightarrow$ anything ν_τ. The ratio of ν_τ over ν_μ fluxes was calculated to be in the 5×10^{-6} range [2], giving a negligible contamination compared to the sensitivity of the experiment.

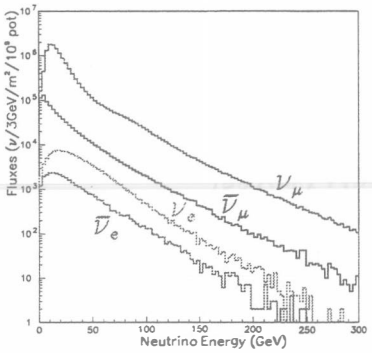

Figure 1: Monte Carlo predictions of the CERN-SPS wide band neutrino beam. Fluxes are given for 10^9 protons on target (p.o.t.).

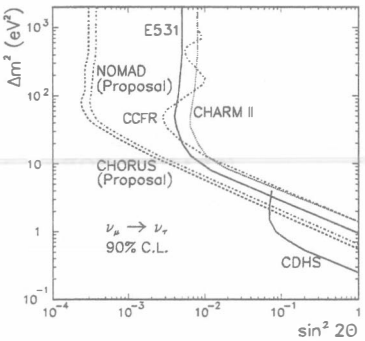

Figure 2: Current 90% C.L. neutrino oscillation parameter limits [3] compared to the limits achievable by the CHORUS and NOMAD experiments.

In the restricted case of two flavor mixing the probability of oscillation as a function of the distance L from the neutrino production point to its interaction point is given by:

$$P = \sin^2(2\theta) \cdot \sin^2(\pi L/\lambda); \quad \lambda[\mathrm{km}] = 2.48 \cdot E[\mathrm{GeV}]/\Delta m^2[\mathrm{eV}^2]$$

where θ is the mixing angle, λ is the oscillation length, E is the neutrino energy and Δm^2 is the neutrino mass squared difference.

NOMAD is especially sensitive to the cosmologically interesting ν_τ mass range: $\Delta m^2 \sim 10 \div 100\ eV^2$. If no evidence for oscillation is found NOMAD is expected to reach the sensitivity limit to oscillation parameters down to 3.8×10^{-4} in $\sin^2 2\theta_{\mu\tau}$ for $\Delta m^2 \geq 40$ eV^2 (Fig. 2).

The selection of ν_τ charged current (CC) interactions in NOMAD relies on kinematic criteria. Thus a careful study of event kinematics, particle isolation and momentum balance (especially in the transverse plane) at the primary vertex allow us to distinguish the ν_τ CC interactions from ν_μ and ν_e CC or neutral current (NC) background events.

Using good measurements of charged particles momenta and total energy flow and the possibility to identify electrons and muons with high efficiency and high purity, NOMAD is able to search for τ^- decays into two leptonic channels: $e^-\nu_\tau\bar{\nu}_e$, $\mu^-\nu_\tau\bar{\nu}_\mu$ and into three hadronic ones: $\pi^-\nu_\tau$, $\rho^-\nu_\tau$ and $\pi^-\pi^-\pi^+ n\pi^0\nu_\tau$, i.e. about 86% of the τ decays.

2 The Detector

A sketch of the NOMAD setup is given in Fig. 3 and a detailed description of the detector can be found elsewhere [4]. We describe briefly its main components. The NOMAD detector consists of a number of subdetectors most of which are located in a dipole magnet with a field volume of $7.5 \times 3.5 \times 3.5\ m^3$. The target part of the detector was designed to accommodate two incompatible requirements: to be as light as possible (low density and low atomic number materials) in order to give precise measurement of charged tracks momenta and to avoid conversions and re-interactions, and to be as heavy as possible to produce a significant number of neutrino interactions.

This compromise was solved using an active target (2.7 tons) of $3 \times 3m^2$ drift chambers (DC) perpendicular to the beam axis, with the target mass given by the chamber structure, a sandwich of honeycomb panels and kevlar-epoxy resin skins. Placed inside the magnetic field of 0.4T, these

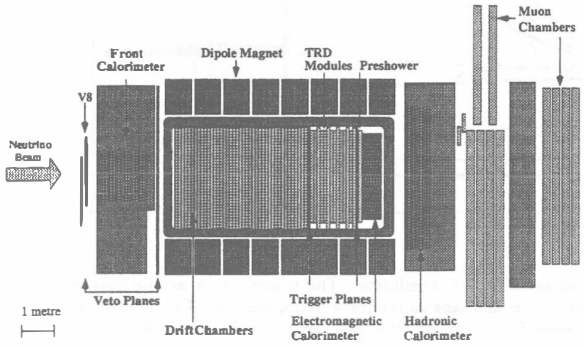

Figure 3: Side view of the NOMAD detector

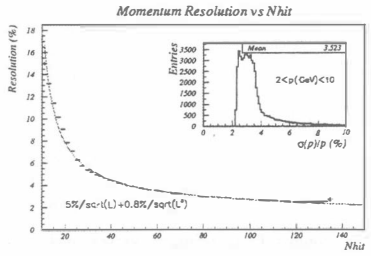

Figure 4: Momentum resolution as a function of the track length (number of hits in the fiducial volume of drift chambers).

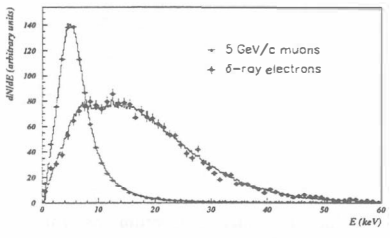

Figure 5: Energy deposition in a TRD straw tube for 5 GeV muons and 2 GeV δ-ray electrons from real data compared to Monte-Carlo (MC) simulation.

chambers provide good position resolution ($< 200\mu$m along the drift direction for incident angles $< 10^0$) and momentum resolution (3.5% in the momentum range $2 < p(\text{GeV}) < 10$) as measured from our 1995 data sample (Fig. 4).

The search for ν_τ events in NOMAD relies strongly on electron and muon identification, as well as on a very accurate determination of the total transverse momentum in an event. The electron identification is performed using the transition radiation detector (TRD). The preshower (PS) and the lead glass electromagnetic calorimeter (ECAL) are used to improve the electron identification and to provide the measurement of its energy as well as the reconstruction of electromagnetic showers induced by photons.

The TRD consists of 9 modules (radiator followed by a detection plane made of straw tubes filled with 80% xenon - 20% methane gas mixture) and provides an π/e rejection factor greater than 10^3 for an electron efficiency of more than 90% for isolated tracks in the momentum range $0.5 < p(\text{GeV}) < 50$. The electron identification in the TRD is based on the difference of energy deposited in the straw tubes by particles of different Lorentz factors $\gamma = E/m$ (Fig. 5).

The preshower is composed of two planes of proportional tubes preceded by a 9 mm (1.6 X_o) lead-antimony (96% - 4%) converter. The electromagnetic calorimeter consists of 875 lead-glass

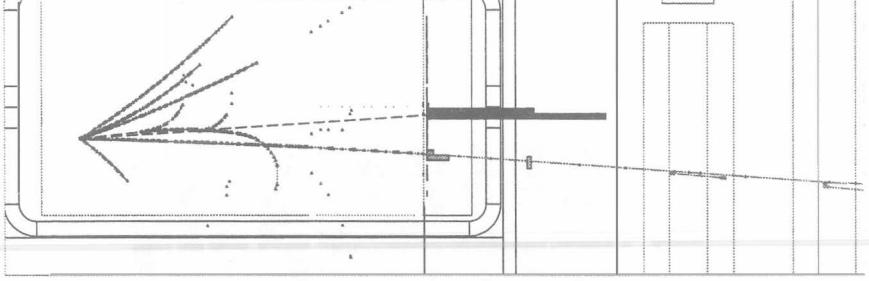

Figure 6: A fully reconstructed ν_μ-CC candidate. The longest track at the bottom is a muon matched to the segments in muon chambers; small triangles are track extrapolations. Two photons (dashed lines) were built: one out of the standalone ECAL cluster, the other from the conversion inside the DC fiducial volume.

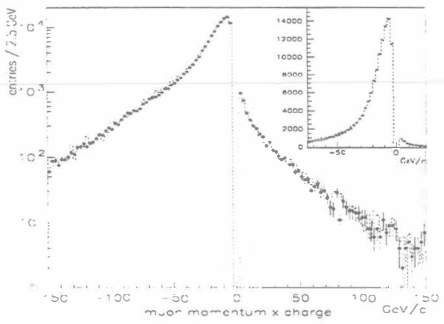

Figure 7: Inclusive muon momentum spectrum signed by the charge of the track.

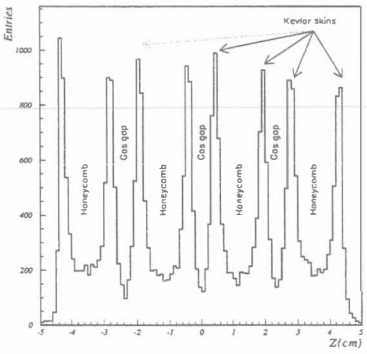

Figure 8: Longitudinal primary vertex distribution folded modulo one chamber. The chamber structure is clearly visible.

Čerenkov counters with a rectangular cross section of $79 \times 112\ mm^2$, 19 radiation lengths deep. The PS and ECAL system provides an additional π/e separation factor of $10^2 - 10^3$ and the energy resolution $\sigma(E)/E = 3.2\%/\sqrt{E(\mathrm{GeV})} \oplus 1\%$.

The iron pillar downstream of the magnet has been instrumented to provide a hadron calorimeter (HCAL) intended to measure neutral hadrons which could generate fake missing momentum in the transverse plane p_T^{miss}. The muon detector is a set of 10 drift chambers arranged in two stations separated by 80 cm thick iron wall. It provides segments and hits which can be associated to extrapolated DC tracks and are used to identify muons or to veto candidate hadrons. Finally, the pillar in front of the magnet has also been instrumented (front calorimeter) to allow a study of multi-muon physics and to search for neutral heavy objects produced in neutrino interactions.

Veto (V) and two trigger planes (T_1 and T_2) are used to select neutrino interactions inside the fiducial volume of the detector with $\bar{V}T_1T_2$ logics.

3 Preliminary analysis

During the 1995 run the NOMAD experiment collected data for a total exposure of 0.62×10^{19} p.o.t. out of which a clean sample of neutrino interactions was selected for detector studies and

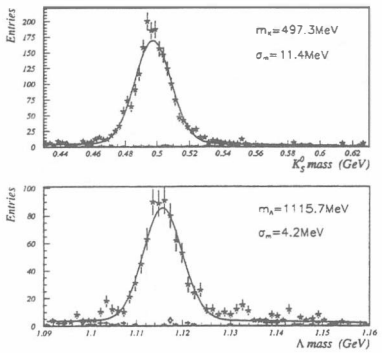

Figure 9: Reconstruction of K^0_s (top) and Λ (bottom) masses in the drift chambers using vertices of $V^0(+-)$ type. Background from the same sign $(++$ and $--)$ combinations is also shown.

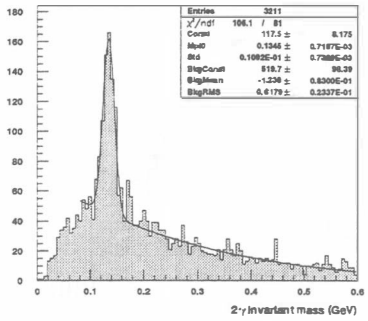

Figure 10: Invariant mass distribution of two photons reconstructed in the electromagnetic calorimeter shows a clear peak from π^0.

preliminary analysis. An example of event reconstruction is given in Fig. 6.

Requiring a primary vertex (with at least two tracks) inside the fiducial volume led to a sample of about 2×10^5 events. Charged current ν_μ and $\bar{\nu}_\mu$ candidates were selected requiring one matched track between the drift chambers and the muon chambers with a momentum larger than 2.5 GeV. The distribution of the muon momentum is shown in Figure 7 together with the Monte Carlo prediction: the agreement is rather good.

Specific studies of the vertex resolution (Fig. 8) and of the K^0_s's, Λ's and π^0's contained in our events (Figs. 9 and 10) were made to control the overall quality of the reconstruction and of the detector performances. We obtained mass resolutions in accordance with our measured (and expected) momentum/energy resolution.

4 Oscillation search

The sensitivity of the experiment in case of no observed signal can be written as

$$P_{osc} < \frac{N_\tau}{(N_\mu/\epsilon_\mu) \times (\sigma_\tau/\sigma_\mu) \times \Sigma_i (Br_i \times \epsilon_i)}$$

where N_τ is an upper limit on the possible number of τ decays, N_μ is the observed number of ν_μ CC interactions inside the fiducial volume, ϵ_μ is the identification efficiency for ν_μ CC events, (σ_τ/σ_μ) the kinematic suppression factor due to the difference in the τ and μ masses, Br_i is the branching ratio and ϵ_i is the selection efficiency for the i-th decay mode of τ.

Using selected events a preliminary oscillation search was performed for the $\tau^- \to e^- \nu_\tau \bar{\nu}_e$, $\tau^- \to \mu^- \nu_\tau \bar{\nu}_\mu$ and $\tau^- \to \pi^- \nu_\tau$ decay channels. Let us consider the last one as an example.

At the first stage events were selected with the following requirements:

- no identified $\mu^\pm$
- no primary $e^\pm$ separated from the hadronic jet
- at least one primary track with negative charge (π^- candidate) capable of reaching the muon detector with momentum $p^\pi > 3$ *GeV*

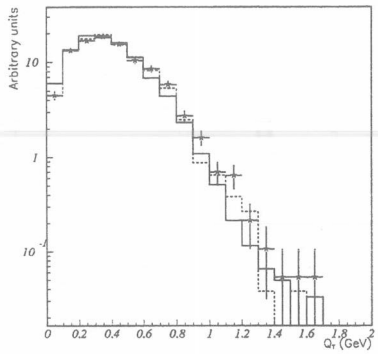

Figure 11: Q_T distributions for NC MC sample (solid line), CC MC events with μ^- removed (dashed line) and "data simulator" (real ν_μ CC events with μ^- removed).

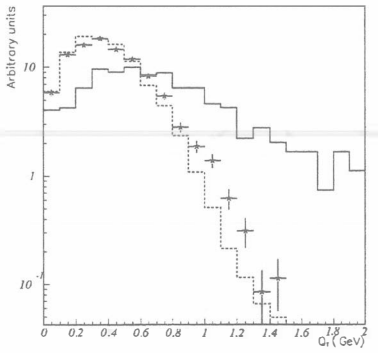

Figure 12: Q_T distributions for simulated $\tau^- \to \pi^-\nu_\tau$ decays (solid line), neutral current background from MC (dashed line) and real data after all cuts applied but Q_T.

- no muon chamber hits in a road along the extrapolated π^- candidate
- energy deposition in ECAL < p^π for this track
- $p^\pi > 0.8 \cdot p^{max}$, where p^{max} is the maximum primary particle momentum (including neutral particles)
- τ consistency, which requires that the $(\pi^-\nu)$ system is consistent with $\tau^- \to \pi^-\nu_\tau$ decay both in
  - transverse plane:
    $(\pi^-\nu)$ transverse mass $M_T < 2.5\,GeV$ $(M_T^2 = (p_T^\pi + p_T^\nu)^2 - (\vec{p_T^\pi} + \vec{p_T^\nu})^2$,where $\vec{p_T^\nu} = \vec{p_T^m})$
  - longitudinal direction:
    p_L^ν calculated from the equation $(E^\nu + E^\pi)^2 - (\vec{p^\pi} + \vec{p^\nu})^2 = m^2$ (where m is the largest between m_τ and M_T) should be less than $40\,GeV$

To reject the background from ν_μ and $\bar{\nu}_\mu$ CC interactions with lost $\mu^\pm$ all events containing a track with the highest p_T which could not reach the muon chambers were removed.

The cut on the transverse momentum component Q_T of the π^- candidate with respect to the total visible momentum $\left(Q_T = \sqrt{(\vec{p^\pi})^2 - (\vec{p^\pi} \cdot \vec{p_{tot}})^2 / p_{tot}^2}\right)$ is imposed in order to reject background from ν NC interactions in which the π^- candidate is a part of the hadronic jet.

The effect of this cut on the samples of simulated ν_μ NC events, simulated ν_μ CC events with muon removed ("fake NC") and "data simulator" (real ν_μ CC events with muon removed) is presented on the Fig. 11. The Q_T distributions for simulated $\tau^- \to \pi^-\nu_\tau$ decays and NOMAD data are shown in Fig. 12.

After the requirement $Q_T > 1.7\,GeV$ we remain with no expected background events and no survivor in real data. The selection efficiency for $\tau^- \to \pi^-\nu_\tau$ is estimated to be $\epsilon(\tau^- \to \pi^-\nu_\tau) = (1.58 \pm 0.18)\%$. Applying the same selection to a sample of simulated $\tau^- \to \rho^-\nu_\tau \to \pi^-\pi^0\nu_\tau$ events we obtain $\epsilon(\tau^- \to \rho^-\nu_\tau) = (0.53 \pm 0.10)\%$.

As a result, using the expected number of ν_μ CC events $(N_\mu/\epsilon_\mu) = 162590$ for normalization and $\epsilon_{\tau\to\pi} \times Br(\tau \to \pi) + \epsilon_{\tau\to\rho} \times Br(\tau \to \rho) = (0.32 \pm 0.03)\%$ we can compute the sensitivity for one prong decay channel $(N_\mu/\epsilon_\mu) \times (\sigma_\tau/\sigma_\mu) \times [\epsilon_{\tau\to\pi} \times Br(\tau \to \pi) + \epsilon_{\tau\to\rho} \times Br(\tau \to \rho)] = 247$.

τ^- search was performed also in a sample of low multiplicity events enriched by quasi-elastic (QE) events and resonance production (RES). The advantage of using this sample compared to the one dominated by deep inelastic scattering (DIS) is a larger (σ_τ/σ_μ) ratio (0.8 instead of 0.48).

Taking into account the other decay channels (Table 1) we can calculate a combined $\nu_\mu \to \nu_\tau$ oscillation limit using the fact that no candidate events were observed in our 1995 data sample while the estimated background amounts to 0.6 events.

Table 1: Sensitivity for studied τ^- decay channels.

Decay channel	**ν interaction type**	$(N_\mu/\epsilon_\mu) \times (\sigma_\tau/\sigma_\mu) \times Br \times \epsilon$
$\tau^- \to e^- \nu_\tau \bar{\nu}_e$	DIS	518
$\tau^- \to e^- \nu_\tau \bar{\nu}_e$	QE + RES	152
$\tau^- \to \mu^- \nu_\tau \bar{\nu}_\mu$	DIS	123
$\tau^- \to \pi^- \nu_\tau$	DIS	247
$\tau^- \to \pi^- \nu_\tau$	QE + RES	218
TOTAL		1258

The uncertainty on the total $\Sigma(N_\mu/\epsilon_\mu) \times (\sigma_\tau/\sigma_\mu) \times Br \times \epsilon$ is about 20%, resulting from the uncertainty on the efficiency calculations. Due to this fact the upper limit on the number of possible τ^- candidates at 90% CL is increased from 2.3 to 2.41 [5].

The preliminary limit on the probability of $\nu_\mu \to \nu_\tau$ oscillations is then:

$$P_{osc}(\nu_\mu \to \nu_\tau) < 2.41/1258 \approx 2 \times 10^{-3}$$

which corresponds to $\sin^2 2\theta_{\mu\tau} < 4 \times 10^{-3}$ for large Δm^2 at 90% CL.

5 Conclusion

It was shown that the NOMAD detector is functioning well. Large sample of data and good resolution allow NOMAD to study a wide area of neutrino physics.

The first preliminary result on the $\nu_\mu \to \nu_\tau$ oscillation search (based on the 1995 data set) was obtained: $\sin^2 2\theta_{\mu\tau} < 4 \times 10^{-3}$ for large Δm^2 at 90% CL. It corresponds to the current best limit from E531 experiment [3]. Nevertheless, significant amount of work is still needed to improve the selection efficiencies (event reconstruction) and the background estimation (event simulation), and also to include analyses of other hadronic decay channels ($\tau \to \rho$ and $\tau \to 3\pi$).

The experimental data from 1996 run are being currently analysed.

The NOMAD detector is ready to continue data taking in 1997.

References

1. NOMAD Collaboration, P. Astier *et al.*, CERN-SPSLC/91-21 (1991); Addendum 1, CERN-SPSLC/91-48 (1991); Addendum 2, CERN-SPSLC/91-53 (1991)
2. M.C. Gonzales-Garcia, J.J. Gomez-Cadenas, CERN-PPE/96-114
3. N. Ushida *et al.*, E531 Collaboration, *Phys. Rev. Lett.* **57**, 2897 (1986). M. Gruwe *et al.*, CHARM-II Collaboration, *Phys. Lett.* B **309**, 463 (1993). K.S. McFarland *et al.*, CCFR Collaboration, *Phys. Rev. Lett.* **75**, 3993 (1995). F. Dydak *et al.*, CDHS Collaboration, *Phys. Lett.* B **134**, 281 (1984).
4. NOMAD Collaboration, To be published in *Nucl. Instrum. Methods* A. Rubbia, *Nucl. Phys.* B **40**, 93 (1995) (Proc. Suppl.). M. Laveder, *Nucl. Phys.* B **48**, 188 (1996) (Proc. Suppl.).
5. R.D.Cousins, V.L.Highland, *Nucl. Instrum. Methods* A **320**, 331 (1992).